

## Nucleotide sugars correlate with leukocyte telomere length as part of a dyskeratosis congenita metabolomic plasma signature

by Yufeng Li, Virág Sághi-Kiss, Emma L.N. James, Inderjeet Dokal, E. Kenneth Parkinson, and Jacob G. Bundy

Received: January 18, 2024.

Accepted: July 26, 2024.

Citation: Yufeng Li, Virág Sághi-Kiss, Emma L.N. James, Inderjeet Dokal, E. Kenneth Parkinson, and Jacob G. Bundy. Nucleotide sugars correlate with leukocyte telomere length as part of a dyskeratosis congenita metabolomic plasma signature.

Haematologica. 2024 Aug 8. doi: 10.3324/haematol.2023.284721 [Epub ahead of print]

### *Publisher's Disclaimer.*

*E-publishing ahead of print is increasingly important for the rapid dissemination of science. Haematologica is, therefore, E-publishing PDF files of an early version of manuscripts that have completed a regular peer review and have been accepted for publication.*

*E-publishing of this PDF file has been approved by the authors.*

*After having E-published Ahead of Print, manuscripts will then undergo technical and English editing, typesetting, proof correction and be presented for the authors' final approval; the final version of the manuscript will then appear in a regular issue of the journal.*

*All legal disclaimers that apply to the journal also pertain to this production process.*

# Nucleotide sugars correlate with leukocyte telomere length as part of a dyskeratosis congenita metabolomic plasma signature

Short title: Metabolomic analysis of dyskeratosis congenita

Yufeng Li,<sup>1</sup> Virág Sági-Kiss,<sup>1</sup> Emma L.N. James,<sup>2</sup> Inderjeet Dokal,<sup>3</sup> E. Kenneth Parkinson,<sup>2</sup> Jacob G Bundy<sup>1\*</sup>

1: Department of Metabolism, Digestion and Reproduction, Imperial College London, Burlington Danes Building, Du Cane Road, London, UK.

2: Centre for Oral Immunology and Regenerative Medicine, Blizard Institute, Barts and the London School of Medicine and Dentistry, Queen Mary University of London, London, UK

3: Centre for Genomics and Child Health, Blizard Institute, Barts and the London School of Medicine and Dentistry, Queen Mary University of London, London, UK.

Author contributions: YL and VSK carried out analytical data acquisition and processing. YL, EKP and JGB carried out statistical analysis. ID was responsible for coordinating clinical sample collection. EKP, EJ, ID, and JGB were responsible for planning and conceptualising the study. All authors read and approved the final draft.

Disclosures: UKRI Natural Environment Research Council (NERC) - NE/S000240/1 EC Horizon 2020 Framework Programme (H2020) - 633589 Dunhill Medical Trust - R452/1115 Barts and the London Charity - MRD&U0004 UKRI Medical Research Council (MRC) - MR/P018440/1 Blood Cancer UK – 14032

Data availability: the data are available from the corresponding author on request.

\*Jake Bundy: [j.bundy@imperial.ac.uk](mailto:j.bundy@imperial.ac.uk)

Dyskeratosis congenita (DC) is a genetically well-characterized telomeropathy.<sup>1,2</sup> There is increasing evidence that senescence is intrinsically linked with changes in metabolism compared to non-senescent cells.<sup>3</sup> We have previously reported that plasma lactate, pyruvate and certain tricarboxylic acid cycle metabolites discriminate DC patients from controls with high significance, independently of glucose levels, chronological age, gender, and disease status.<sup>4</sup> Here, we present a broader profiling analysis using an LC-MS-MS-based targeted metabolomics strategy, with no overlap in terms of detected metabolites with our earlier study. While targeted metabolomics is, by definition, limited to detecting only metabolites that are known *a priori*, it provides high-quality<sup>5</sup> data that are well suited to clinical and translational research.

We analysed a set of plasma samples taken from 29 DC patients and 30 matched controls. The study was approved by the London-City and East Research Ethics Committee (reference 07/Q0603/5). The cohorts were age-matched, with a mean of  $38 \pm 17$  (SD) years for the control samples, and  $37 \pm 17$  for the patient samples (P value, Welch's t test, 0.81). Further details of the patients are given as supplementary files by James et al.<sup>4</sup> We used a combined amine derivatization and ion pairing chromatography analytical strategy, which gives broad metabolome coverage including highly polar metabolites.<sup>6</sup>

In total, we detected 146 metabolites, following filtering for quality. Thirty-one of these were significantly different at a significance cutoff of  $P < 0.01$ ; 16 and 11 of these remained significant following correction for false discovery rate (1%), and Bonferroni correction, respectively. In particular, the nucleotide sugars uridine diphosphate glucose (UDPG) and adenosine diphosphate ribose (ADPR) combined highly significant P values with the largest fold changes of any of the metabolites (Figure 1A). (It should be noted that UDP-glucose was not chromatographically distinguished from the structural isomer UDP-galactose by our analytical method, and therefore the signal may contain contributions from both metabolites; similarly, 2-phosphoglycerate and 3-phosphoglycerate were also not chromatographically separated.) Inspection of the individual metabolites showed, as expected, clear differences between the two groups (Figure 1B). Furthermore, an unsupervised multivariate analysis (principal components analysis, PCA) showed a clear difference between the healthy and DC patient samples along PC 1, and a supervised linear discriminant analysis (LDA) was an excellent classifier, with an area under the receiver operating characteristic (ROC) curve of 0.98 (Figure 2A,B). Indeed, selecting as few as three metabolite biomarkers was sufficient to give near-complete separation of the two groups (Figure 1D). We believe that there is significant potential to use metabolite analysis to help inform diagnosis of DC.

The DC signature was independent of age and gender. We constructed logistic regression models with disease status as the dependent variable, and age + sex + metabolite as independent variables. These showed that the P values (from effect likelihood ratio tests) were essentially unaffected by age and gender, generally lying along  $x=y$  when comparing the two models (i.e. logistic regression against DC alone, versus DC + age + sex). The only metabolite with a substantial difference between the two was UDPG, and this was actually *more* significant with the additional variables (age and sex) than without. For the top 9 metabolites (i.e. those still significant after Bonferroni correction) all metabolites still had  $P < 0.0001$  with respect to DC status.

We also analysed the effect of sample age (i.e. length of storage in -80 freezer, not patient age) on metabolites. The control samples consisted of two groups: "old" (i.e. collected roughly

contemporaneously with the DC samples), and “new” (collected more recently). The results were highly comparable whether analysing “old” control samples only against DC, or whether analysing the combined old + new control group against DC (data not shown). In addition, we also analysed the effect of sample age for the control samples alone. Most metabolites were highly stable (as shown by lack of significant change with respect to sample age), and furthermore, comparing the significant metabolites with and without the new sample age group showed that the pattern of separation according to DC was basically unchanged. We therefore excluded just two metabolites, where the effect of the sample age was similar to the effect of DC (iminodiacetic acid, and cysteinylglycine). The nucleotide sugars showed no evidence for association with sample age ( $P = 0.39$  and  $0.33$  for UDPG and ADPR, respectively).

While there were some associations between metabolites and other, potentially confounding clinical parameters (available for DC patients only), only ornithine of the highly significant metabolites showed a weak relationship with platelet count (Table S2;  $P = 0.04$  and MCV  $P = 0.006$ ). We also carried out an analysis of sub-groups; if patients with lung disease, liver disease, or skin symptoms are removed from the analysis, then the 9 most significant metabolites all remain highly significant, indicating that the differences are not just down to these potential confounders (Table 1). Several metabolites correlated with age-associated leukocyte telomere length (AALTL) (available for 18 of the DC group of patients only; Table S1). While we do not have data on other cell/tissue types, all tissues analyzed in DC have shorter age-associated telomere lengths (AATLs) than normal.<sup>7</sup> Furthermore, in *TERT* and *TERC* knockout mice, postmitotic tissues inherit shorter telomeres and display telomere dysfunction and progeroid phenotypes,<sup>8</sup> but leukocyte AATL may still be an indicator of systemic telomere dysfunction. In particular, the sugar nucleotides UDPG and ADPR were again distinguished from all other metabolites by their high correlation with AALTL (Figure 1C; Pearson’s  $R = -0.65$  and  $-0.60$ , respectively). This gives us confidence that the associations for these two compounds are real and biologically meaningful, in that we see within-group quantitative effects of telomere length, and not just differences between control and patient samples. In addition, in order to check that this association between UDPG and ADPR with AALTL was not confounded by other clinical parameters (white blood cell count, platelet count, mean corpuscular volume, haemoglobin, presence of skin symptoms), we analysed the data by regression against telomere length and each other parameter in turn, i.e. metabolite concentration =  $f(\text{AALTL} + \text{parameter} + \text{AALTL} \times \text{parameter})$ . The AALTL term was significant ( $p < 0.05$ ) for all ten additional models, i.e. five clinical parameters and two metabolites (Table 1).

Importantly, all the 9 highly significant metabolites remained highly significant when only the *TERC* mutated group were considered (Table S1) arguing strongly against proposed extrachromosomal functions of telomerase affecting the metabolite levels. Analysis of the metabolite data showed no clear effect of mutation locus (supplementary information, Figure S1). However, single sample pathway analysis (SSPA) has recently been introduced as a novel approach for analysis of metabolomic data: the data are transformed from the metabolite space into a pathway space, which can provide additional power for revealing biological phenotypes.<sup>9</sup> An unsupervised multivariate analysis (PCA) of the SSPA-transformed data shows, indeed, that the phenotypic separation that we see is subtly different from that of the raw data, and potentially very interesting. For example, the main separation between control and DC samples dropped down from PC 1 to PC 4 ( $P = 7.2 \times 10^{-7}$ , t test); and there was a very clear difference

between males and females on PC 2 ( $P = 1.9 \times 10^{-6}$ , t test). Therefore, we also carried out SSPA-PCA on the DC data alone, in order to look for possible differences between mutation sub-types. There were some possible differences between subtypes, as shown by an unsupervised analysis (Figure 2C); using the supervised LDA (with an initial dimension reduction step to the first 3 PCs), then there was a clearer separation between DKC against the TERC/TERT mutation groups, which were overlapping (Figure 2D; area under the ROC curve for DKC group = 0.98).

Several of the metabolic alterations detected in DC have potential significance for the role of telomeres in human ageing and age-related conditions. It is tempting to look at the changes in ADPR, in particular, and conjecture a link to poly (ADP-ribose) polymerase activity. Five of the ADP-ribose transferase (ART) family have clear roles in genome maintenance and are involved in telomere biology.<sup>10</sup> Perhaps the changes in free ADPR are simply reflecting changes in overall ADP ribosylation. This, however, ignores the fact that UDPG is altered similarly to ADPR, both in terms of direction and amount of change, and therefore we think the changes in nucleotide sugars are more likely to be indicative of a broader biochemical change – for instance, a change in the balance between anabolism and catabolism.

Of further interest it has recently been reported that serum taurine levels decline in parallel with human chronological age and that taurine protects against telomere loss in fish but does not affect telomerase activity in fish or mice.<sup>11</sup> There were no changes in plasma taurine or hypotaurine levels in DC patients versus controls, suggesting telomere disruption is unlikely to drive taurine depletion in adult humans. Aspartate and sarcosine accumulation are associated with sarcopenia<sup>12</sup>, which is linked to frailty; if we also consider metabolites significant at a FDR of 5% (Table S2), this then also covers beta-hydroxyisovalerate, which is depleted in sarcopenia.<sup>13</sup> Hydroxylysine accumulation is associated with collagen degradation,<sup>14</sup> which is implicated in wrinkles; ascorbate is also essential for collagen production, and this is also significantly different, although actually increased in the DC group. Most interesting of all the depletion of four neuroprotective metabolites (hydroxykynurenine,<sup>15</sup> kynurenine,<sup>15</sup> N-acetylleucine,<sup>16</sup> norvaline and paraxanthine<sup>17</sup>) as well as paradoxically three neurotoxic ones (N-acetylisoleucine, quinolate<sup>15</sup> and quinolate carboxylate<sup>15</sup>) was observed in DC patient plasma, indicating a possible link between telomere dysfunction and neuronal function. Many of these metabolites have been linked with other telomeropathies such as ataxia telangiectasia,<sup>16</sup> in addition to Alzheimer's Disease, Parkinson's Disease and amyotrophic lateral sclerosis.

## References

1. Tummala H, Walne A, Dokal I. The biology and management of dyskeratosis congenita and related disorders of telomeres. *Expert Rev Hematol.* 2022;15(8):685-696.
2. Revy P, Kannengiesser C, Bertuch AA. Genetics of human telomere biology disorders. *Nat Rev Genet.* 2023;24(2):86-108.
3. Wiley CD, Campisi J. The metabolic roots of senescence: mechanisms and opportunities for intervention. *Nat Metabolism.* 2021;3(10):1290-1301.
4. James EN, Sagi-Kiss V, Bennett M, et al. Dyskeratosis Congenita Links Telomere Attrition to Age-Related Systemic Energetics. *J Gerontol A Biol Sci Med Sci.* 2023;78(5):780-789.
5. Begou O, Gika HG, Wilson ID, Theodoridis G. Hyphenated MS-based targeted approaches in metabolomics. *Analyst.* 2017;142(17):3079-3100.
6. Sagi-Kiss V, Li Y, Carey MR, et al. Ion-Pairing Chromatography and Amine Derivatization Provide Complementary Approaches for the Targeted LC-MS Analysis of the Polar Metabolome. *J Proteome Res.* 2022;21(6):1428-1437.
7. Gadalla SM, Cawthon R, Giri N, Alter BP, Savage SA. Telomere length in blood, buccal cells, and fibroblasts from patients with inherited bone marrow failure syndromes. *Aging (Albany NY).* 2010;2(11):867-874.
8. Sahin E, Colla S, Liesa M, et al. Telomere dysfunction induces metabolic and mitochondrial compromise. *Nature.* 2011;470(7334):359-365.
9. Wieder C, Lai RPJ, Ebbels TMD. Single sample pathway analysis in metabolomics: performance evaluation and application. *BMC Bioinformatics.* 2022;23(1):481.
10. Muoio D, Laspata N, Fouquerel E. Functions of ADP-ribose transferases in the maintenance of telomere integrity. *Cell Mol Life Sci.* 2022;79(4):215.
11. Singh P, Gollapalli K, Mangiola S, et al. Taurine deficiency as a driver of aging. *Science.* 2023;380(6649):eabn9257.
12. Calvani R, Picca A, Marini F, et al. A Distinct Pattern of Circulating Amino Acids Characterizes Older Persons with Physical Frailty and Sarcopenia: Results from the BIOSPHERE Study. *Nutrients.* 2018;10(11):1691.
13. Oktaviana J, Zanker J, Vogrin S, Duque G. The Effect of  $\beta$ -Hydroxy- $\beta$ -Methylbutyrate (HMB) on Sarcopenia and Functional Frailty in Older Persons: A Systematic Review. *J Nutr Health Aging.* 2018;23(2):145-150.

14. Sato M, Sasaki M, Nagai Y. Increased urinary excretion of collagen metabolites in cadmium-metallothionein nephropathy. *Arch Toxicol.* 1987;61(2):116-119.
15. Fathi M, Vakili K, Yaghoobpoor S, et al. Dynamic changes in metabolites of the kynurenine pathway in Alzheimer's disease, Parkinson's disease, and Huntington's disease: A systematic Review and meta-analysis. *Front Immunol.* 2022;13:997240.
16. Saberi-Karimian M, Beyraghi-Tousi M, Mirzadeh M, Gumprich E, Sahebkar A. The Effect of N-Acetyl-DL-Leucine on Neurological Symptoms in a Patient with Ataxia-Telangiectasia: a Case Study. *Cerebellum.* 2023;22(1):96-101.
17. Yoo C, Xing D, Gonzalez D, et al. Acute Paraxanthine Ingestion Improves Cognition and Short-Term Memory and Helps Sustain Attention in a Double-Blind, Placebo-Controlled, Crossover Trial. *Nutrients.* 2021;13(11):3980.

Table 1. The metabolites most significantly associated with dyskeratosis congenita and with telomere length remain significant, even when excluding patients with lung disease, liver disease, or skin symptoms (for all 9 metabolites significant after Bonferroni correction), or allowing for the other clinical parameters listed in this table (for the nucleotide sugars UDP-glucose and ADP-ribose only).

Metabolite	P values for metabolites calculated for sub-groups				P values for metabolite association with telomere length, including other clinical factors as possible confounders					
	No lung disease; DC n=23	No liver disease; DC n=24	Neither liver nor lung disease; DC n=22	No skin symptoms; DC n=14	None	White blood cell count	Platelet count	Mean corpuscular volume	Haemoglobin	Presence of skin symptoms
	DC N =23	DC N =24	DC N = 22	DC N=14						
ADP-ribose <sup>a</sup>	2.1 x 10 <sup>-6</sup>	2.6 x 10 <sup>-5</sup>	2.2 x 10 <sup>-6</sup>	0.01	0.0088	0.0036	0.014	0.0087	0.0061	0.0033
Alanylglycine <sup>a</sup>	1.5 x 10 <sup>-6</sup>	1.2 x 10 <sup>-7</sup>	2.7 x 10 <sup>-7</sup>	0.002						
Ornithine <sup>a</sup>	1.9 x 10 <sup>-7</sup>	4.4 x 10 <sup>-7</sup>	7.9 x 10 <sup>-7</sup>	9.9 x 10 <sup>-6</sup>						
Paraxanthine <sup>b</sup>	0.0002	0.0002	0.0005	0.008						
Phosphoglycerate <sup>a</sup>	3.7 x 10 <sup>-6</sup>	1.7 x 10 <sup>-6</sup>	2.1 x 10 <sup>-6</sup>	0.003						
Quinolate <sup>b</sup>	2.5 x 10 <sup>-6</sup>	1 x 10 <sup>-5</sup>	6.2 x 10 <sup>-6</sup>	0.004						
Sarcosine <sup>a</sup>	7.8 x 10 <sup>-8</sup>	3.2 x 10 <sup>-7</sup>	1.1 x 10 <sup>-7</sup>	0.0008						
UDP-Glucose <sup>a</sup>	7.3 x 10 <sup>-9</sup>	7.9 x 10 <sup>-9</sup>	7.7 x 10 <sup>-9</sup>	2.3 x 10 <sup>-6</sup>	0.0039	0.0049	0.0095	0.0087	0.0061	0.0046
Xanthine <sup>a</sup>	1 x 10 <sup>-5</sup>	2.1 x 10 <sup>-5</sup>	2.9 x 10 <sup>-5</sup>	7.9 x 10 <sup>-6</sup>						

a: metabolites increased in DC

b: metabolites decreased in DC



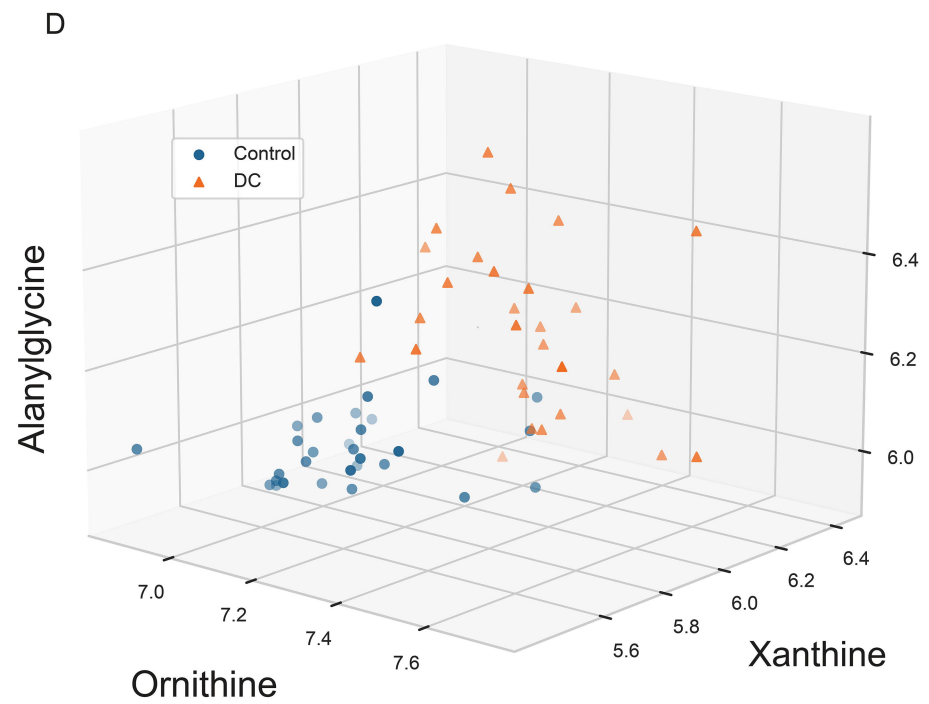
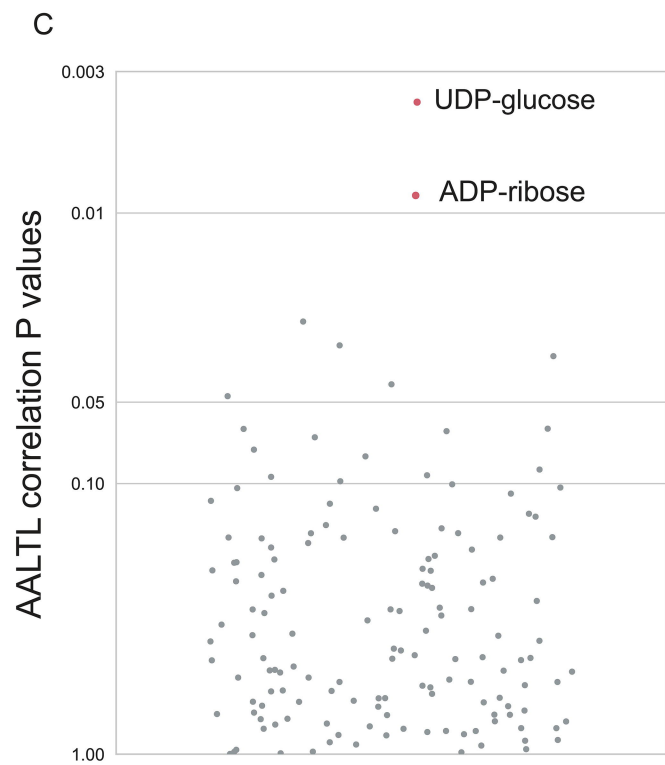
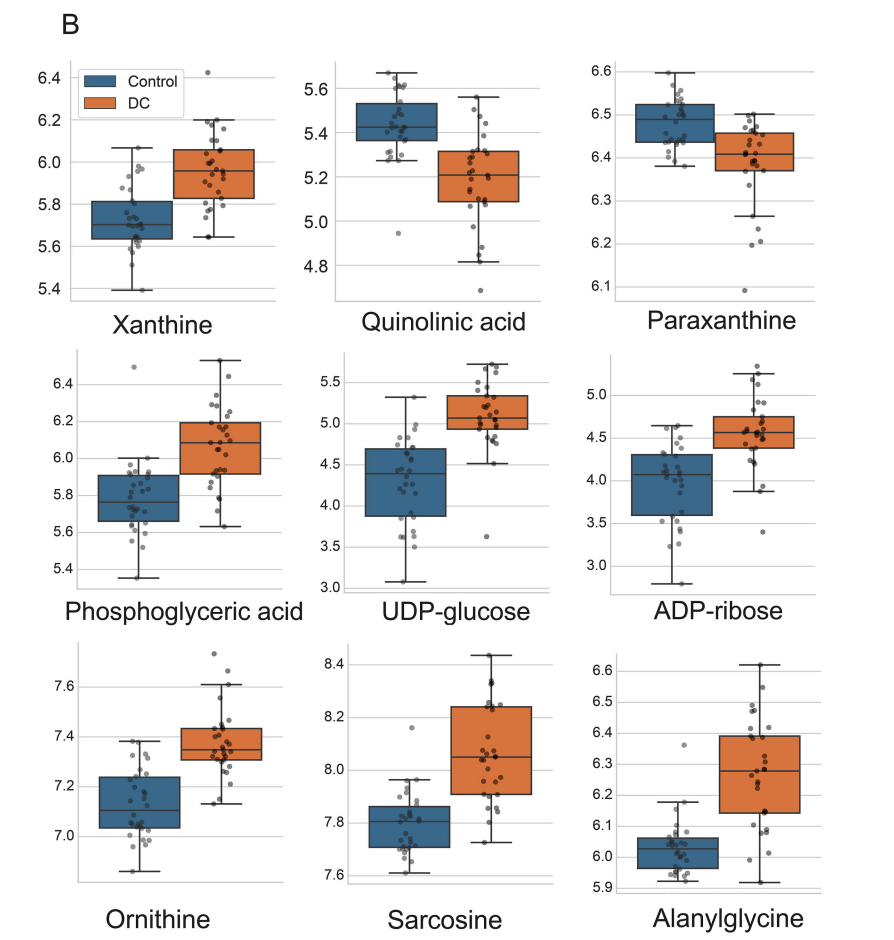
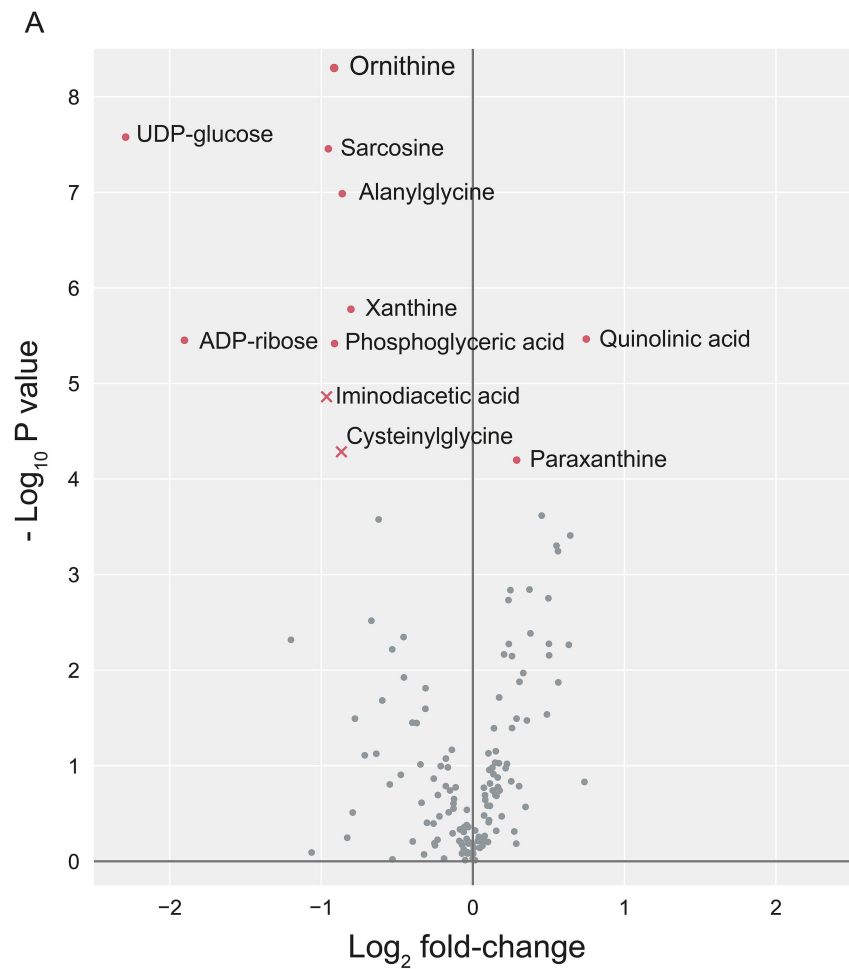
## Figure Legends.

**Figure 1.** Individual metabolites discriminate dyskeratosis congenita patient from control samples with high accuracy.

- A: Volcano plot shows fold-change (abscissa) against P value (t test, log-transformed data). Eleven metabolites are significant following Bonferroni correction and are named on the plot, although two (cysteinylglycine, iminodiacetic acid – points marked by crosses) are not considered further because of potential analytical problems. The nucleotide sugars ADP-ribose and UDP-glucose are distinguished from all other metabolites by the magnitude of the fold-change.
- B: Differences between healthy and DC patient groups for individual metabolites (only metabolites significant following Bonferroni correction are shown here).
- C: The nucleotide sugars ADP-ribose and UDP-glucose are distinguished from all other metabolites on the basis of their correlation with age-adjusted leukocyte telomere length (AALTL; data for DC patients only): P value from correlation shown on Y axis. (X axis does not represent any data, and is used purely to prevent point overlap: the points are ordered randomly.)
- D: Three metabolites are sufficient to provide near-complete separation of disease classes.

**Figure 2.** Multivariate analyses distinguish both disease from control, and mutational sub-groups.

- A: Unsupervised principal components analysis (PCA) of scores plot shows clear difference between DC patient and control samples along PC 1.
- B: Supervised linear discriminant analysis (LDA; following initial dimension reduction to first 10 PCs by PCA) demonstrates excellent classification into groups (area under receiver operating characteristic curve = 0.98).
- C: Unsupervised PCA following single-sample pathway analysis (SSPA-PCA) demonstrates potential metabolic pathway differences between disease mutation loci: PCs 1-3 are shown.
- D: Supervised LDA shows classification of disease sub-types on the basis of metabolic pathway differences, following dimension reduction by SSPA-PCA (PCs 1-3).



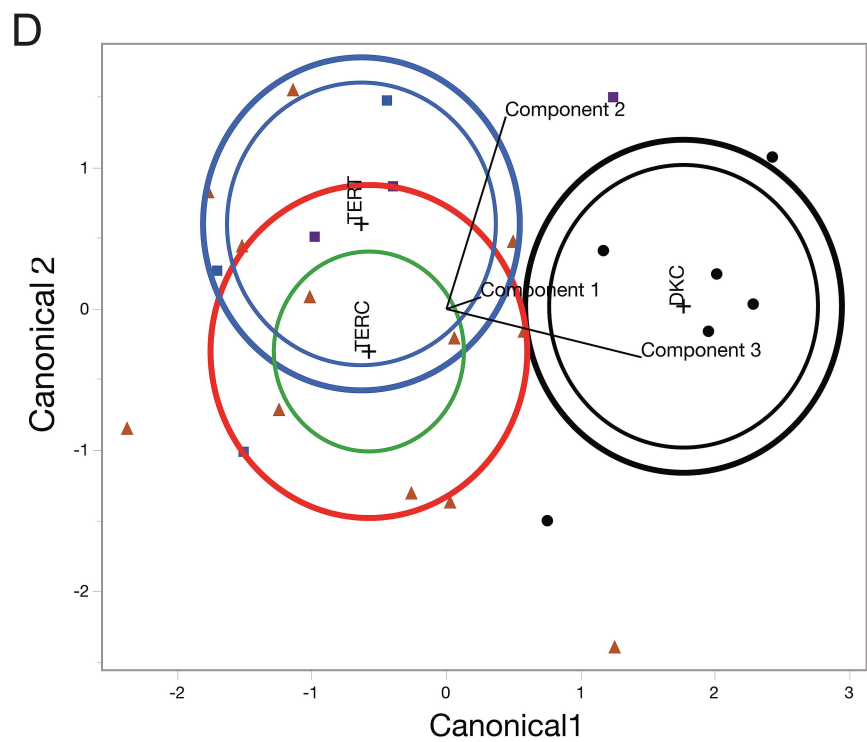
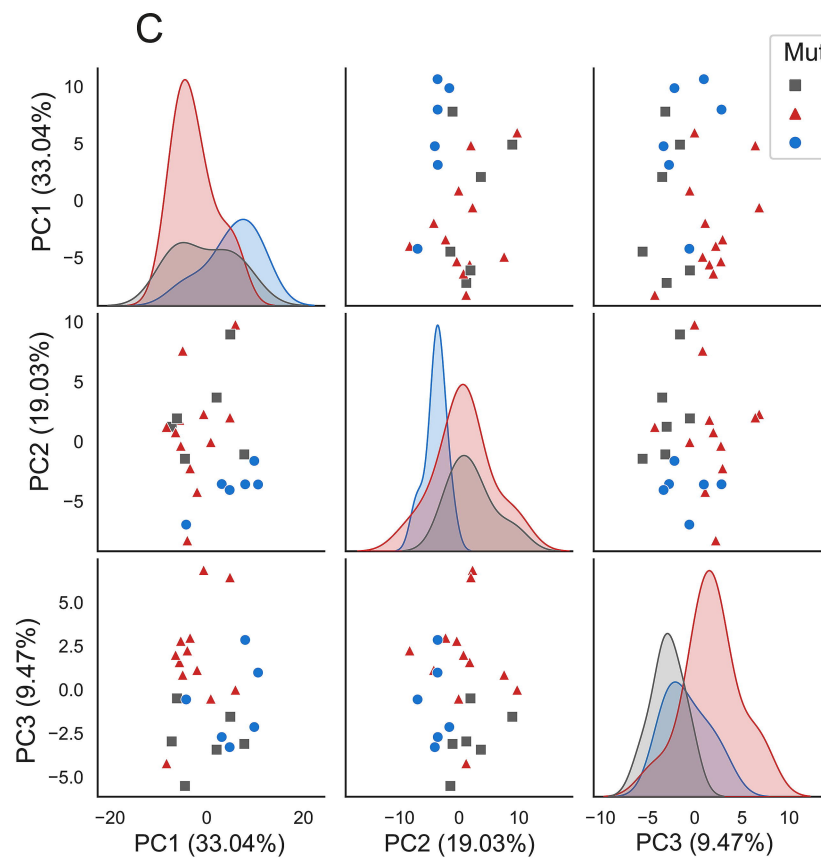
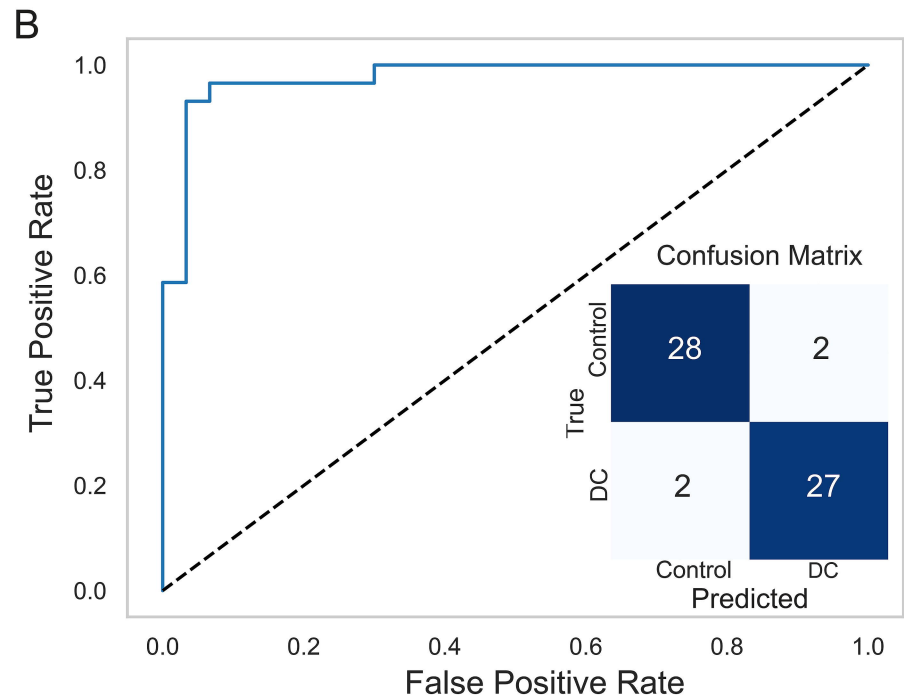
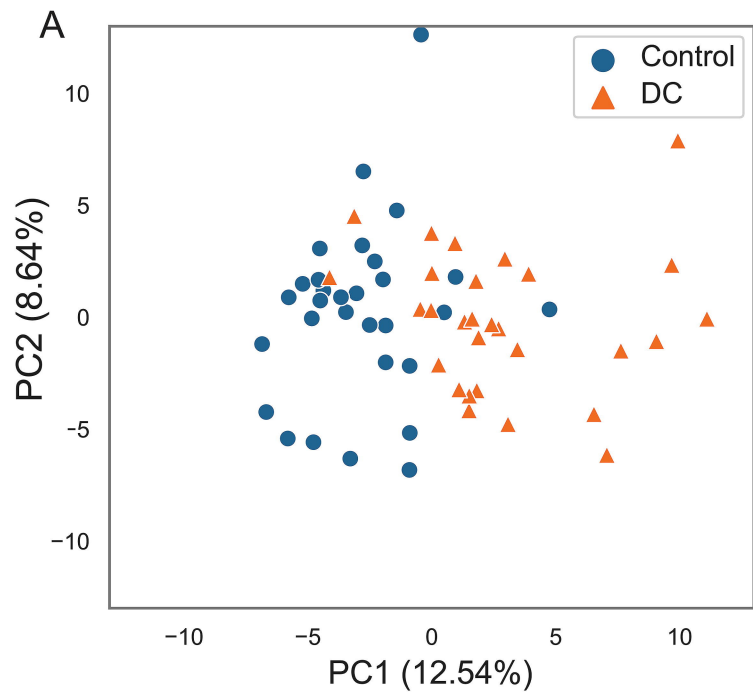


**Table S1. Summary of metabolites distinguishing DC patients from control subjects: relationship to AATL and TERC only mutants.**

Metabolite	P Value Rank Test <sup>a</sup>	P Value Welch's T test	Chronological Age Link	TERC Mutants only (n =12) <sup>a</sup>
1,2,3 Propane TCA	0.002	0.006		0.01
5-Aminopentanoate	0.02	0.04		0.04
Acetylalanine	0.0002	0.002		0.002
Acetylleucine	0.002	0.0007	Depletion linked to neurodegeneration <sup>1,2</sup>	0.0008
ADMA	0.0007	0.02	Increases with cardiovascular risk <sup>3</sup>	0.34
ADP ribose	0.0001	8.9 x 10 <sup>-5</sup>		0.02
Alanylglycine	3.5 x 10 <sup>-7</sup>	7.8 x 10 <sup>-7</sup>		0.00007
Allantoin	0.0008	0.002	Yes Inhibitor of collagenase <sup>4</sup>	0.0001
Argenine	0.003	0.001	Depletion associated with Alzheimer's Disease <sup>5</sup>	0.04
Ascorbate	0.0008	0.006	Declines with age and associated with frailty. May also be protective against cognitive decline <sup>6</sup>	0.007
Aspartate	0.0009	3 x 10 <sup>-5</sup>	Yes	0.003
Beta Alanine	0.009	0.01		0.04
Beta hydroxyisovaleric acid	0.0045	0.003	Yes muscle deterioration <sup>7</sup>	0.002
Cinnamic Acid	0.03	0.02	Antioxidant protects against skin ageing <sup>8</sup>	0.25
CMP	0.0009	0.01		0.05
Cystine	0.009	0.007	Oxidative defence protects against hippocampus degeneration <sup>9</sup>	0.1
Cytidine	0.01	0.01		0.11
Deoxyuridine	0.005	0.03		0.0005
Glycerate	0.002	0.0007	Yes <sup>10</sup>	0.04
Hydroxykynurenine	0.002	0.0007	Depletion and increase linked to neurodegeneration <sup>11</sup>	0.004

Hydroxylysine	0.0007	0.01	Yes Collagen Degradation <sup>12</sup>	0.004
Hypoxanthine	0.000008	0.04	Yes <sup>10</sup>	0.69
Indoleacetate	0.006	0.003	Yes <sup>10</sup>	0.10
Kynurenine	0.004	0.006	Depletion linked to neurodegeneration Alzheimer's and Parkinson's <sup>11</sup>	0.32
N-acetylalanine	0.0001	0.002	Yes <sup>10</sup>	0.03
N-acetylleucine	0.0003	0.0007	Depletion linked to neurodegeneration <sup>1,2</sup>	0.04
N-acetylisoleucine	0.002	0.002	Yes cognitive function	0.02
N-acetylneuraminic acid	0.049	0.05	Increase linked to neurodegeneration	0.01
N-Formyl-L-methionine	0.035	0.045		0.05
N-methylglutamate	0.002	0.001		0.004
Phosphoglycerate <sup>c</sup>	0.00002	0.00004	Pentose phosphate pathway	0.0006
Nor-valine	0.01	0.01	Depletion associated with Alzheimer's Disease <sup>13</sup>	0.84
Ophthalmate	0.002	0.005		0.03
Ornithine	<6 x 10 <sup>-7</sup>	1.5 x 10 <sup>-8</sup>	Yes	0.000009
Paraxanthine	0.0002	9 x 10 <sup>-5</sup>	Yes Depletion linked to neurodegeneration <sup>14</sup>	0.008
Quinate	0.03	0.125		1.0
Quinolate	0.000009	6.4 x 10 <sup>-6</sup>	Accumulation linked to neurodegeneration and immunosuppression <sup>15</sup>	0.007
Quinolate Carboxylate	0.01	0.02	Accumulation linked to neurodegeneration and immunosuppression <sup>15</sup>	0.12
S-Adenosyl methionine	0.04	0.03	Yes Enhances ageing Substrate for methylation.	0.001

Sarcosine	<6 x 10 <sup>-7</sup>	1.7 x 10 <sup>-7</sup>	Frailty Sarcopenia <sup>16</sup> Caloric restriction Macroautophagy <sup>17</sup>	0.00004
Trans-4-hydroxyproline	0.02	0.02	Collagen degradation <sup>18</sup>	0.65
Tryptamine	0.02	0.06		0.15
UDP-Glucose <sup>d</sup>	<6 x 10 <sup>-7</sup>	1.7 x 10 <sup>-7</sup>	Frailty, Cognitive Decline <sup>19</sup>	0.00006
Uridine monophosphate	0.006	0.005	Age-related cognitive decline <sup>20</sup>	0.004
Xanthine	0.000006	2.5 x 10 <sup>-6</sup>	Yes <sup>10</sup>	0.0004
Xanthurenate	0.01	0.02	Depletion linked to Alzheimer's Disease and Ageing <sup>21</sup>	0.06

<sup>a</sup> Wilcoxon-Mann-Whitney Test; <sup>c</sup> 2-phosphoglycerate and 3-phosphoglycerate were not resolved by our analytical method; <sup>d</sup> may also contain contributions from UDP-galactose, if present.

- Hegdekar, N., Lipinski, M. M. & Sarkar, C. N-Acetyl-L-leucine improves functional recovery and attenuates cortical cell death and neuroinflammation after traumatic brain injury in mice. *Sci Rep* **11**, 9249, doi:10.1038/s41598-021-88693-8 (2021).
- Kaya, E. *et al.* Acetyl-leucine slows disease progression in lysosomal storage disorders. *Brain Commun* **3**, fcaa148, doi:10.1093/braincomms/fcaa148 (2021).
- Raimondi, L. *et al.* n-3 polyunsaturated fatty acids supplementation decreases asymmetric dimethyl arginine and arachidonate accumulation in aging spontaneously hypertensive rats. *Eur J Nutr* **44**, 327-333, doi:10.1007/s00394-004-0528-5 (2005).
- Marzook, F., Marzook, E. & El-Sonbaty, S. Allantoin may modulate aging impairments, symptoms and cancers. *Pak J Pharm Sci* **34**, 1377-1384 (2021).
- Kan, M. J. *et al.* Arginine deprivation and immune suppression in a mouse model of Alzheimer's disease. *J Neurosci* **35**, 5969-5982, doi:10.1523/JNEUROSCI.4668-14.2015 (2015).
- Lewis, L. N. *et al.* Lower Dietary and Circulating Vitamin C in Middle- and Older-Aged Men and Women Are Associated with Lower Estimated Skeletal Muscle Mass. *J Nutr* **150**, 2789-2798, doi:10.1093/jn/nxaa221 (2020).
- Oktaviana, J., Zanker, J., Vogrin, S. & Duque, G. The Effect of beta-hydroxy-beta-methylbutyrate (HMB) on Sarcopenia and Functional Frailty in Older Persons: A Systematic Review. *J Nutr Health Aging* **23**, 145-150, doi:10.1007/s12603-018-1153-y (2019).
- Hseu, Y. C. *et al.* Trans-cinnamic acid attenuates UVA-induced photoaging through inhibition of AP-1 activation and induction of Nrf2-mediated antioxidant genes in human skin fibroblasts. *J Dermatol Sci* **90**, 123-134, doi:10.1016/j.jdermsci.2018.01.004 (2018).
- Verbruggen, L. *et al.* Lifespan extension with preservation of hippocampal function in aged system x(c)(-)-deficient male mice. *Mol Psychiatry* **27**, 2355-2368, doi:10.1038/s41380-022-01470-5 (2022).
- Menni, C. *et al.* Metabolomic markers reveal novel pathways of ageing and early development in human populations. *Int J Epidemiol* **42**, 1111-1119, doi:10.1093/ije/dyt094

dyt094 [pii] (2013).

- 11 Fathi, M. *et al.* Dynamic changes in metabolites of the kynurenine pathway in Alzheimer's disease, Parkinson's disease, and Huntington's disease: A systematic Review and meta-analysis. *Front Immunol* **13**, 997240, doi:10.3389/fimmu.2022.997240 (2022).
- 12 Sato, M., Sasaki, M. & Nagai, Y. Increased urinary excretion of collagen metabolites in cadmium-metallothionein nephropathy. *Arch Toxicol* **61**, 116-119, doi:10.1007/BF00661368 (1987).
- 13 Polis, B., Srikanth, K. D., Gurevich, V., Gil-Henn, H. & Samson, A. O. L-Norvaline, a new therapeutic agent against Alzheimer's disease. *Neural Regen Res* **14**, 1562-1572, doi:10.4103/1673-5374.255980 (2019).
- 14 Yoo, C. *et al.* Acute Paraxanthine Ingestion Improves Cognition and Short-Term Memory and Helps Sustain Attention in a Double-Blind, Placebo-Controlled, Crossover Trial. *Nutrients* **13**, doi:10.3390/nu13113980 (2021).
- 15 Moffett, J. R. *et al.* Quinolate as a Marker for Kynurenine Metabolite Formation and the Unresolved Question of NAD(+) Synthesis During Inflammation and Infection. *Front Immunol* **11**, 31, doi:10.3389/fimmu.2020.00031 (2020).
- 16 Calvani, R. *et al.* A Distinct Pattern of Circulating Amino Acids Characterizes Older Persons with Physical Frailty and Sarcopenia: Results from the BIOSPHERE Study. *Nutrients* **10**, doi:10.3390/nu10111691 (2018).
- 17 Walters, R. O. *et al.* Sarcosine Is Uniquely Modulated by Aging and Dietary Restriction in Rodents and Humans. *Cell Rep* **25**, 663-676 e666, doi:10.1016/j.celrep.2018.09.065 (2018).
- 18 Reed, A. D. *et al.* The Stickland Reaction Precursor trans-4-Hydroxy-L-Proline Differentially Impacts the Metabolism of *Clostridioides difficile* and Commensal Clostridia. *mSphere* **7**, e0092621, doi:10.1128/msphere.00926-21 (2022).
- 19 Kameda, M., Teruya, T., Yanagida, M. & Kondoh, H. Frailty markers comprise blood metabolites involved in antioxidation, cognition, and mobility. *Proc Natl Acad Sci U S A* **117**, 9483-9489, doi:10.1073/pnas.1920795117 (2020).
- 20 Cummings, J. *et al.* Effect Size Analyses of Souvenaid in Patients with Alzheimer's Disease. *J Alzheimers Dis* **55**, 1131-1139, doi:10.3233/JAD-160745 (2017).
- 21 Sathyaikumar, K. V. *et al.* Xanthurenic Acid Formation from 3-Hydroxykynurenine in the Mammalian Brain: Neurochemical Characterization and Physiological Effects. *Neuroscience* **367**, 85-97, doi:10.1016/j.neuroscience.2017.10.006 (2017).

<b>Table S2. The relationship of DC patient metabolites to clinical indicators and the age of control samples.</b>						
Metabolite	WBC <sup>a</sup>	Platelets <sup>a</sup>	Hb <sup>a</sup>	MCV <sup>a</sup>	Patients with skin symptoms <sup>b</sup>	Recent v Old Controls <sup>b</sup>
Alanylglycine	0.85	0.14	0.41	0.75	0.68	0.002+
Allantoin	0.09	0.002	0.06	0.71	0.50	0.67
Beta hydroxyisovaleric acid	0.27	0.003	0.42	0.07	0.20	0.05
Cystathionine	0.66	0.29	0.25	0.62	0.0042	0.81
Deoxyuridine	0.08	0.001	0.68	0.82	0.15	0.50
Hydroxylysine	0.3	0.2	0.51	0.4	0.63	0.04+
Kynurenine	0.28	0.8	0.16	0.94	0.47	0.02
N-acetylalanine+	0.69	0.77	0.42	0.005+	0.44	0.12
N-acetylleucine	0.3	0.02	0.95	0.95	0.58	0.08
N-acetylneuranimine	0.008	0.002	0.45	0.06	0.69	0.72
N-methylglutamate	0.98	0.66	0.88	0.48	0.042	0.86
Ornithine	0.08	0.04	0.06	0.006	0.014	0.10
S-Adenosyl methionine	0.28	0.006	0.3	0.005	0.32	0.99
Sarcosine	0.58	0.95	0.96	0.46	0.67	2.24E-05+
Trans-4-hydroxyproline	0.73	0.95	0.41	0.05	0.0057	0.42
Xanthurenate	0.63	0.42	0.05	0.73	0.74	0.01

<sup>a</sup>Linear regression analysis; <sup>b</sup> Wilcoxon-Mann-Whitney Test; <sup>c</sup> 2-phosphoglycerate and 3-phosphoglycerate not distinguishable by analytical method; <sup>d</sup> potential interferences from UDP-galactose.

+ Going in the opposite direction from DC and therefore indicating the true difference between DC and control subjects may be greater than indicated.